Unsteady Aerodynamics for Wind Turbine Blades Using State Space Formulation

M. Sayed [a], A. El-Badawy [b]

[a] *German University in Cairo, Cairo, Egypt, mohammed.sayed@guc.edu.eg*
[b] *Mechanical Engineering Department, Al-Azhar University, Cairo, Egypt and German University in Cairo, Cairo, Egypt, ayman.elbadawy@guc.edu.eg*

1 ABSTRACT

Dynamic stall is a critical phenomenon which has an important effect on the operation of Horizontal Axis Wind Turbines (HAWT). In this paper, the Unsteady Reynolds-Averaged Navier-Stokes (URANS) method with transition Shear Stress Transport (SST) turbulence model is used to capture the dynamic stall of an oscillating HAWT blade profile. To be able to capture the unsteady effect of wind on the blade, a Kaimal turbulence power spectral density model has been used. The results obtained from the numerical simulations are used to determine the coefficients of a semi-empirical dynamic stall state-space model of a two-dimensional airfoil section. This model includes four state variables. Two state variables are used to model the unsteady lift for attached flow conditions, and another two are used to model the dynamics of trailing edge separation. The state-space model can later be integrated with structural dynamics model for aeroelastic simulations.

2 INTRODUCTION

Dynamic stall has been widely known to significantly affect the performance of a large variety of fluid machinery, such as helicopter crafts, highly maneuverable fighters, gas turbines, and wind turbines. It has been well recognized that the dynamic stall process can be categorized into four key stages, i.e. attached flow at low angles of attack, development of the Leading Edge Vortex (LEV), the shedding of the LEV from the suction surface of the blade and the reattachment of the flow (Marcus, Matthies, 2004). Although the basic image of the phenomenon has been generally clarified, the physics of this strongly non linear unsteady flow phenomenon has not yet been completely understood and more efforts are needed to advance the knowledge to the level on which we could accurately predict and precisely control the dynamic stall. Most of the previous researches have investigated flows at high Reynolds number ($Re \geq 10^6$) or high Mach number ($Ma \geq 0.3$) which falls into the compressible flow regime. However, dynamic stall at low Reynolds number has distinct features compared with those at high Reynolds number, such as flow transition process, laminar separation and reattachment, etc. Moreover, the wind turbine application falls into low Reynolds number range.

In recent years, Navier-Stokes numerical solvers have been used to determine airfoil loads under dynamic stall situations (Hansen et. al., 2004; Larsen et. al., 2007). Due to the extensive cost of these calculation, practical applications doesn't seem within a near future, but solving the Navier-Stokes equations gives an insight into the flow and pressure changes occurring during a dynamic stall cycle. It should be noticed that larger discrepancies between numerical and experimental results seems to be accepted within the so-called semi-empirical models than for the Navier-Stokes solver. The goals of the semi-empirical models are not to capture every variation in the load, but to model the main characteristics in a fast and efficient way. The main drawback

of the semi-empirical models is that all of them are dependent on available static data and use interpolation into tabulated values or curve fitting techniques to determine quasi-static lift values. A semi-empirical model should be able to reproduce these static values for quasi-static rates of the angle of attack, i.e. $\dot{\alpha} \approx 0$.

The aim of the present paper is to use computational fluid dynamics (CFD) calculations utilizing the URANS with transition SST turbulence model to capture the dynamic stall of a wind turbine oscillating blade. The calculations were performed at low Reynolds number flows ($\approx 10^5$). The CFD calculations provide a detailed two-dimensional analysis and hence gain a better understanding of the flow phenomenon. A semi-empirical dynamic stall model of a two-dimensional blade section is then devised. The model includes 4 state variables describing important contributions as regards the aerodynamics of wind turbine blades. The model uses two state variables to describe the dynamic lift under attached flow conditions, and another two are used to model the dynamics of trailing edge separation. Leading edge separation and the dynamics between the travelling and trailing edge vortices are disregarded in this model.

3 NUMERICAL SIMULATION

3.1 *Case studied*

The 2D airfoil employed in the numerical calculations is an S809 airfoil which is a special purpose airfoil for HAWT developed by the National Renewable Energy Laboratory (NREL, 2010). The airfoil with a chord length of *c=1m*, which the in this case executes sinusoidal pitching motion $\alpha = \alpha_{mean}° + \Delta\alpha° \sin(\omega t)$ around an axis located at a quarter of its chord (0.25c) from the leading edge with a reduced frequency $k = \omega c / U_\infty = 0.057$. The stream velocity following Kaimal distribution (Leishman, 2006) with a mean speed of U_∞=7 m/s is shown in Figure 1.

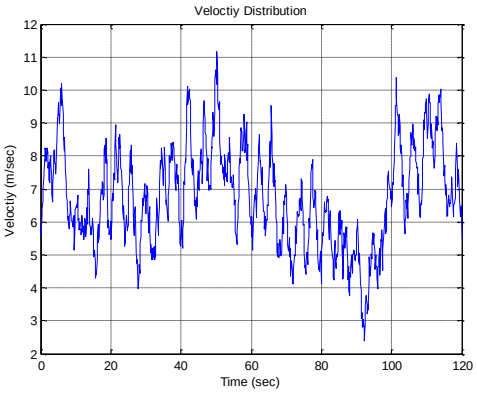

Figure 1 velocity distribution generated using Kaimal turbulence power spectral density model

3.2 *Numerical Technique*

In this study, a 2D model has been created by ANSYS CFX software (ANSYS Inc, 2010). The simulations are performed using URANS method which is numerically less expensive than Detached Eddy Simulation (DES). The turbulence model used in this type of numerical simulations is the transition SST model, which is a choice that makes a good compromise in the lift prediction (Shengyi et al., 2010).

3.3 *Grid design*

The geometry of the airfoil is imported as point coordinates that define the airfoil profile. The airfoil has a chord length equal to 1m and its leading edge is located 10m from the domain inlet, whereas the flow domain consists of a 30m x10m parallelogram. Due to the inability of CFX to

simulate 2D cases(ANSYS Inc, 2010), the flow domain along with the airfoil itself is created as an extrusion of unit length. The produced parallelepiped will then be meshed with a single element depth so that the third dimension is diminished, and the top and bottom faces of the extrusion will be set as symmetry planes later in the process.

The grid generation for the proposed numerical study is shown in Figure 2a. In near wall regions, the velocity gradients produced by boundary layer phenomena need elements with high aspect ratios, in order to be resolved in a computationally efficient manner. For this reason, the mesh implemented used prisms to create a mesh that is finely resolved normal to the wall but coarse parallel to it, by inflating the 2D local face elements into 3D prism elements. In the present case study, this inflation was applied on the airfoil surface in order to take into account the effect of the boundary layer on its aerodynamic behavior. The parameters that control the inflation were carefully chosen in order to capture the flow phenomena within the boundary layer, such as transition or separation (Figure 2b).

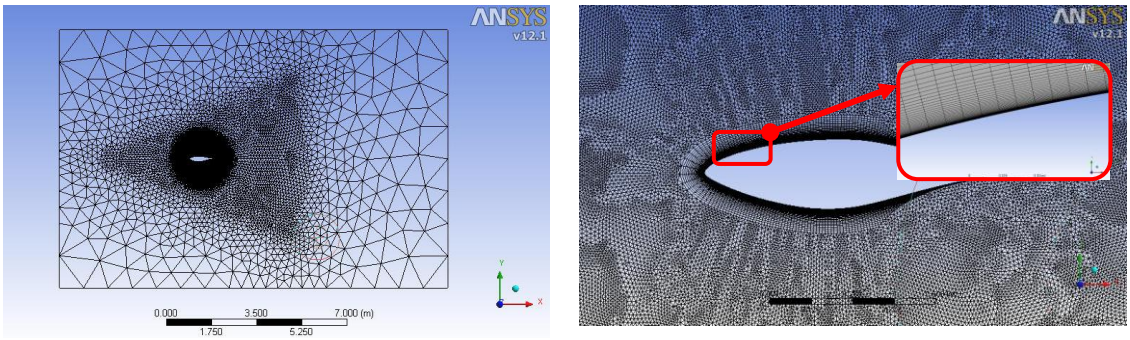

(a) (b)

Figure 2 (a) The grid generation of the flow domain (b) Zoom on the mesh near the airfoil surface

3.4 *Transition SST turbulence model*

The transition SST Model is a four-equation turbulence model which is based on the coupling of the SST *k-ω* transport equations with two other transport equations, one for the intermittency and the other for the transition onset criteria, in terms of the momentum-thickness Reynolds number. This is a reasonably new model and it is expected to predict flows with massive separations more accurately. For further details on the transition SST Model, see 0(Shengyi et al., 2010; ANSYS Inc, 2010).

3.5 *CFD results*

Before discussing the flow development, it should be noted that due to the oscillating motion of the airfoil, the fluid particles adjacent to the airfoil should always have the same local velocities as that of the airfoil wall. Therefore, strictly speaking, there is no fully attached flow in this situation, even at very low angles of attack, for example $\alpha \approx 2°\uparrow$, as shown in Figure 3a, even though the main flow is basically 'attached' to the airfoil profile there still exists a very thin separation layer due to the above-mentioned reason. However, as one can observe, this kind of separation is normally so thin that it does not affect the flow field and therefore, it can be ignored. Figure 3 shows the velocity distribution and streamlines over an S809 airfoil at the attached and separated flow regimes and at a specified oscillating angle of attack. Moreover, the effect of the oscillation in the attached flow regime is almost the same during either pitching up or pitching down. In the early stage of the upstroke phase, $2° \leq \alpha \leq 6°$, the flow is fully attached to the airfoil in the sense of ignoring the thin separation layer.

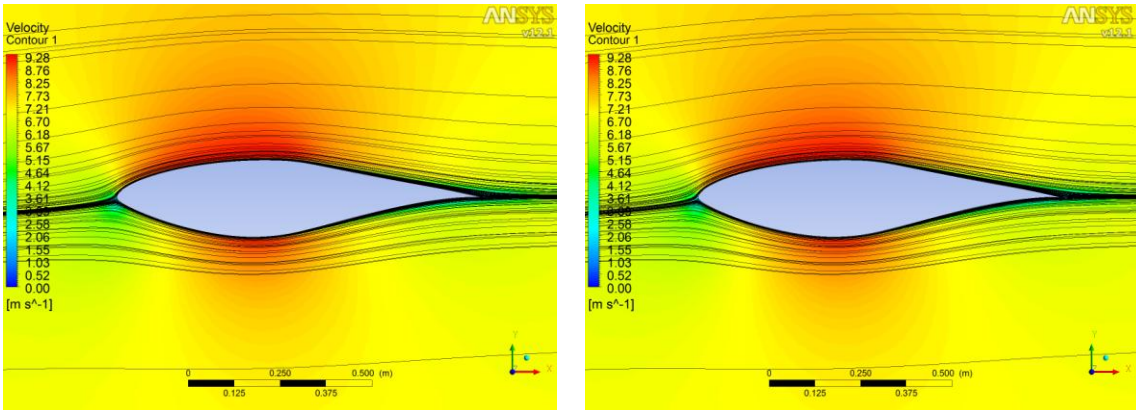

(a) (b)

Figure 3 Velocity fields superimposed on the instantaneous streamlines at $\alpha = 2°$ for oscillation of $\alpha = 4° + 2° \sin(0.4t)$ (a) Blade pitching up. (b) Blade pitching down.

Figure 4 shows the detachment of the LEV, as well as the flow separations due to the vortices in the stall region. As shown in Figure 4a, at $\alpha \approx 15°\uparrow$, the trailing edge vortex has grown and the LEV becomes very weak. Then the airfoil comes to the down stroke phase. The vortices on the airfoil begin to emerge together and only one large vortex can be seen at $\alpha \approx 15°\downarrow$ as shown in Figure 4b.

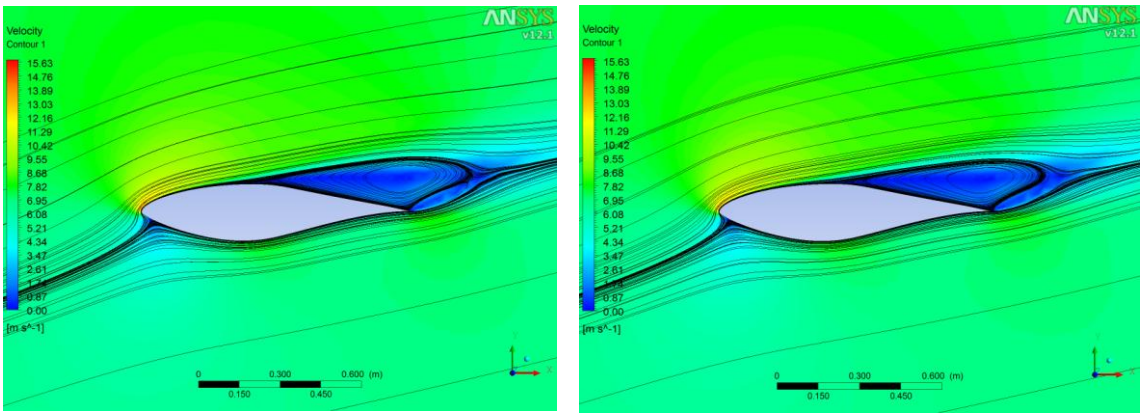

(a) (b)

Figure 4 Velocity fields superimposed on the instantaneous streamlines at $\alpha = 15°$ for oscillation of $\alpha = 16° + 3° \sin(0.4t)$ (a) Blade pitching up. (b) Blade pitching down.

During stall ($13° \leq \alpha \leq 19°$), at the maximum angle of attack of $\alpha \approx 19°$, it turns out to be two vortices close to the trailing edge at the airfoil suction side as shown in Figure 5a. This is due to the development of a tiny separation bubble close to the leading edge. Considering the low Reynolds number circumstances in this study, this bubble is actually the so-called Laminar Separation Bubble (LSB) (Shengyi et al., 2010) in which the flow turbulence intensity is significantly enhanced and this causes a turbulent boundary layer to appear after the LSB as shown in Figure 5b. The lift coefficient C_L was determined by integrating the pressure distribution over the airfoil surface.

Figure 6 shows the steady and the unsteady C_L at the different flow regimes. The steady C_L is also calculated using ANSYS CFX. Despite the flow is attached in this regime, the unsteady lift coefficient in both cases is below that of the static value during the oscillation of the blade profile as shown in Figure 6a which is mainly due to the delay on the onset of the flow separation under the unsteady conditions.

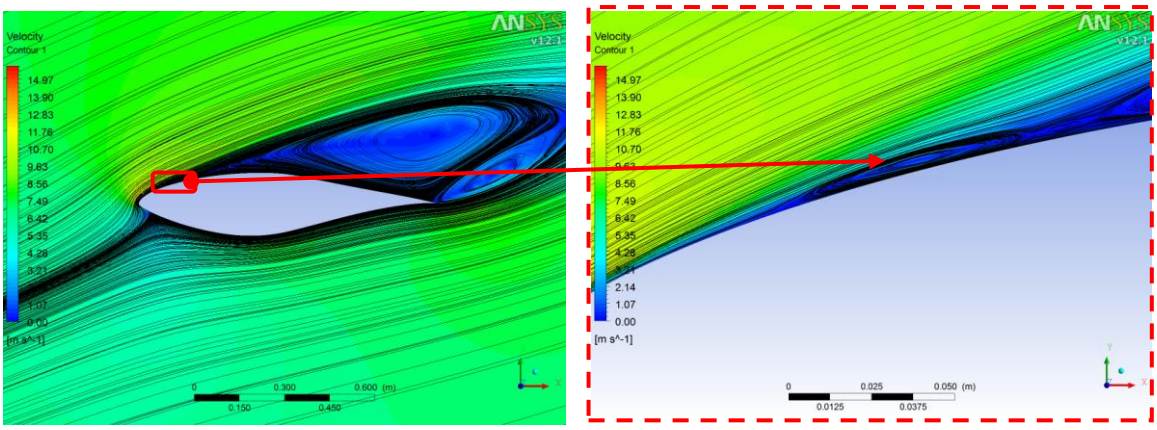

(a) (b)

Figure 5 Flow field at α = 19° for oscillation of α = 16°+ 3° sin (0.4t) (a) LEV (b) Zoom at the Leading edge to show the LSB

This delay can be explained as follows: by increasing the angle of attack, the unsteadiness of the flow resulting from circulation that is shed into wake at the trailing edge of the airfoil causes a reduction in lift and adverse the pressure gradient compared to the static value. In addition, in response to the external pressure gradients, there are also additional unsteady effects that occur within the boundary layer, including the existence of flow reversals in the absence of any significant flow separation. During the stall regime, the dynamic lift coefficient values are above that of the static values when the blade pitching up and slightly below when it is pitching down (Figure 6b). Finally, the unsteady C_L data points are used to find out the state space coefficients as described in section 4.

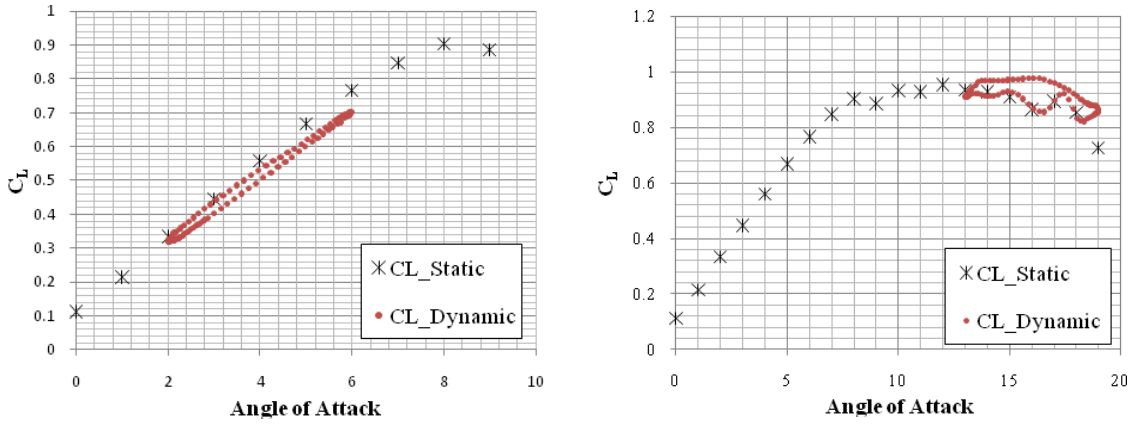

(a) (b)

Figure 6 The static versus dynamic lift coefficient distribution results from Ansys CFX (a) α = 4°+ 2° sin (0.4t). (b) α = 16°+ 3° sin (0.4t).

4 STATE SPACE FORMULATION

The dynamics of the aerodynamic system is related to the lift, and the unsteady drag and pitching moment are then determined from the unsteady lift. For wind turbines, Mach number are lower than 0.3 and it is assumed that the flow is incompressible. For the attached flow the leading edge separation is assumed not to be a dominating phenomenon and the model will be given by Theodorsen theory (Theodorsen, 1935), and only trailing edge separation is considered under stalled flow conditions. There are different types of the dynamic stall state space models such as: The Beddoes-Leishman, Øye, Risø, ONERA and Boeing-Vertol models (Leishman, 2000; Hansen et. al., 2004). The Risø model is the used model in this work. In which, a closed set of nonlinear or-

dinary differential equations of the dynamic stall model are implemented and then used to determine the dynamic airfoil data (lift, drag, and moment coefficient).

The Risø model developed by Hansen et al. (Hansen et. al., 2004) at Risø National Laboratory, Denmark, is a modified version of the Beddoes-Leishman model using only 4 state variables. Two state variables are used to model the unsteady lift for attached flow conditions, and another two are used to model the dynamics of trailing edge separation. Leading edge separation and the dynamics between the travelling and trailing edge vortices are disregarded in this model. Assuming knowledge of the separation point and the lift under fully attached flow and fully separated flow conditions, respectively, the total static lift coefficient C_L is given by:

$$C_L = fC_{L0} + (1-f)C_{L1} \tag{1}$$

where C_{L1} is the viscous lift coefficient under both attached and separated regimes. The lift coefficient of the profile under fully attached flow is denoted C_{L0} which it is found from the lift slope at α_0, and the position of the separation point given by f is evaluated from equation (2).

$$C_L \cong \left(\frac{1+\sqrt{f}}{2}\right)^2 C_{L0} \tag{2}$$

The restriction is that if f as determined from equation (2) is larger than 1.0, it is set equal to 1.0, and when full separation occur, f is set equal to 0. From a given set of static C_L data using ANSYS CFX, f is found from equation (2) and C_{L1} may be determined from equation (1). Inverting equation (1) creates a singularity at $f = 1$, i.e. at fully attached flows. Under such conditions C_{L1} is set to half the linear lift, i.e. C_{L1} ($f = 1$) = $C_{L0}/2$. To introduce dynamic effects f and C_{L0} is modified. Under fully attached flow conditions the Risø model works on a modified angle of attack instead of directly on the linear lift. The dynamic angle of attack α_d is given as:

$$\alpha_d(t) = \alpha(1 - A_1 - A_2) + c_1(t) + c_2(t) \tag{3}$$

Where,

$$\dot{c}_i + \left(\omega_i + \frac{\dot{U}}{U}\right)c_i = \omega_i A_i \alpha \qquad i = 1,2 \tag{4}$$

Now the dynamic linear lift is evaluated as,

$$C_{L0,d} = C_{L0}(\alpha_d) + \frac{\pi c \dot{\alpha}}{2U} \tag{5}$$

where A_i and ω_i are profile dependent variables describing the time delay. For a thin profile in incompressible flow the values of A_1 and A_2 will be determined from the numerical analysis, ω_1 and ω_2 represents the timescale for low and high frequency rotations, respectively. To introduce dynamic effects on the separation point motion the same approach as the Beddoes-Leishman (Leishman, 2000; Hansen et. al., 2004) model is used. A retarded linear lift $C'_{L0}(t)$ is introduced as a delayed state variable of the linear lift $C_{L0,d}(t)$, which should give a one-to-one correspondence between the pressure coefficient and the dynamic lift at changing pitch rates (equation 6).

$$\dot{C}'_{L0,d}(t) = -\omega_3\left(C'_{L0,d}(t) - C_{L0,d}(t)\right) \tag{6}$$

An effective angle of attack, $\alpha_f = C_{L0}/\, dC_L/d\alpha|_{\alpha 0} + \alpha_0$ is then used to find the actual static attachment degree by which f_d can be found from equation 7.

$$\dot{f}_d(t) = -\omega_4\left(f_d(t) + f(\alpha_f)\right) \tag{7}$$

This introduces additional 2 state variables C'_{L0} and f_d. In state space formulation the Risø may be written as follows:

$$\dot{x} = Ax + b \tag{8}$$

Where,

$$x=\begin{bmatrix} c_1 \\ c_2 \\ C'_{L0} \\ f_d \end{bmatrix}, \qquad A=\begin{bmatrix} -\left(\omega_1+\frac{\dot{U}}{U}\right) & 0 & 0 & 0 \\ 0 & -\left(\omega_2+\frac{\dot{U}}{U}\right) & 0 & 0 \\ 0 & 0 & -\omega_3 & 0 \\ 0 & 0 & 0 & -\omega_4 \end{bmatrix}, \qquad b=\begin{bmatrix} \omega_1 A_1 \alpha \\ \omega_2 A_2 \alpha \\ \omega_3\left(C_{L0}(\alpha_d)+\frac{\pi c\dot{\alpha}}{2U}\right) \\ \omega_4 f(\alpha_f) \end{bmatrix}$$

Finally, the dynamic lift coefficient can be determined from,

$$C_{L,d}(t)=f_d(t)C_{L0}(\alpha_d)+(1-f_d(t))C_{L1}(\alpha_d) \tag{9}$$

The values of A_1, A_2, $\omega_{1..4}$ are determined such that the dynamic model would fit the dynamic lift coefficient. The total unsteady lift on the airfoil under the attached and stalled flow conditions will then be determined by simultaneous solution of the state equations (8). The model proposed here was produced for harmonic rotation of the airfoil at various mean angle of attack, the amplitude $\Delta\alpha$ and the reduced frequency $k = \omega c/ U_\infty$ are kept constant, where c is the chord length of the profile set equal to 1 m, U_∞ is the undisturbed incoming wind velocity equal to 7 m/s and ω is the rotational frequency of oscillation.

The state-space model used in this article solves each regime separately. Figure 7 shows the effects of increasing the angle of attack, while holding the reduced frequency constant at k = 0.057. These results show the effects on the air loads as the flow state progresses from nominally attached conditions at the lowest mean angle, through "light" dynamic stall as shown in Figure 7a, and into "deep" dynamic stall for the highest mean angle as shown in Figure 7b. the results from the state-space model shows good agreement with the results obtained by the CFD model.

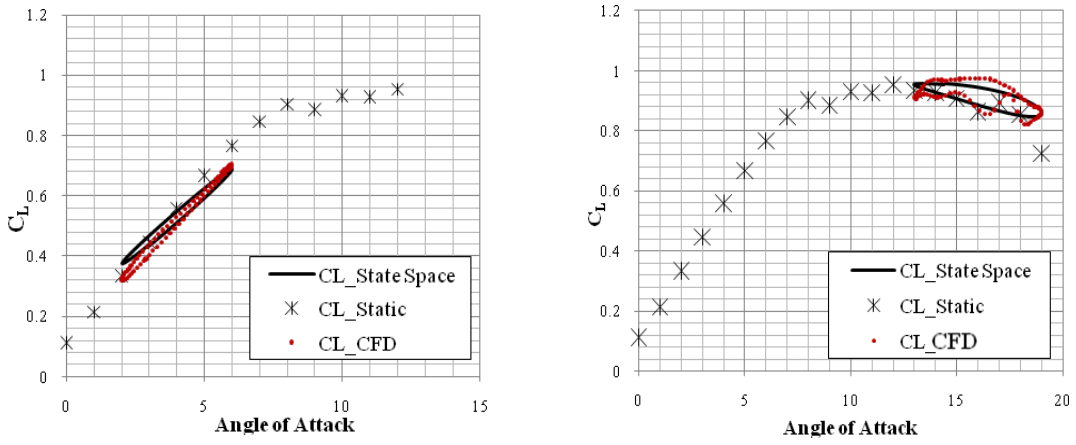

Figure 7 The static versus dynamic lift coefficient distribution results from Ansys CFX compared to state space model (a) α = 4°+ 2° sin (0.4t). (b) α = 16°+ 3° sin (0.4t).

The profile dependent variables describing the dynamic response during the oscillation in the attached regime and the stalled regime are tabulated in Table 1. These variables were chosen in order to make the dynamic response from the state-space formulation fit the response obtained from the CFD simulation. Modification on the model to obtain the dynamic response in both regimes is advised for the future work.

Table 1. Profile dependent parameters for the state-space dynamic stall model

Oscillation	A_1	A_2	ω_1	ω_2	ω_3	ω_4
α = 4°+ 2° sin (0.4t)	0.15	0.2	0.2	0.01	0.1	0.8
α = 16°+ 3° sin (0.4t)	0.6	0.05	0.2	0.01	0.1	0.8

5 CONCLUSIONS

In this work, URANS with the transition SST turbulence model has been employed to simulate the unsteady fluid flow around S809 airfoil executing a sinusoidal pitching, in the low Reynolds number fluid flow regime. The steady and unsteady C_L is obtained using the CFD model and then the unsteady C_L data points were used to find out the state-space coefficients. A state-space model was then devised to fit CFD simulations. The effect of the oscillation in the attached flow regime is almost the same during either pitching up or pitching down. In addition, the unsteady lift coefficients in the both cases were found to be similar to the static values during the oscillation of the blade profile in the attached flow regime. Furthermore, during the stalled regime the lift coefficients are higher than the static values when the blade is pitching up and slightly less than the static values when it is pitching down. This state-space model can later be integrated with structural dynamics model for aeroelastic simulations.

6 ACKNOWLEDGEMENTS

The authors would like to acknowledge the financial support from the Science and Technology Development Fund (STDF), Cairo, Egypt under grant number 1495.

7 REFERENCES

ANSYS Inc, "ANSYS CFX 12.1 (Theory Guide)," 2010.

http://wind.nrel.gov/.

Hansen, M. H., Gaunaa, M., and Madsen, H. A., 2004. A Beddoes-Leishman type dynamic stall model in state-space and indicial formulations. Risø-r-1354(en), Risø National Laboratory, Roskilde, Denmark.

J. Gordon Leishman, 2006. Principles of Helicopter. Cambridge University Press.

J.W. Larsen, S.R.K. Nielsen, S. Krenk, 2007. Dynamic stall model for wind turbine airfoils. Journal of Fluids and Structures 23, 959–982.

Marcus Meyer, Hermann G. Matthies, 2004. State-space representation of instationary two-dimensional airfoil aerodynamics. Journal of Wind Engineering and Industrial Aerodynamics vol. 92, pp. 263–274.

Shengyi Wang, Lin Ma, Derek B Ingham, Mohamed Pourkashanian and Zhi T., 2010. Turbulence Modelling of Deep Dynamic Stall at Low Reynolds Number. WCE 2010, June 30 - July 2, London, U.K.

Theodorsen, T., 1935. General Thoery of Aerodynamic Instability and the Mechanism of Flutter. NACA report 496, pp. 413 433.